JACS
JOURNAL OF THE AMERICAN CHEMICAL SOCIETY
Article
Cite This: J. Am. Chem. Soc. 2018, 140, 17071−17078
pubs.acs.org/JACS

Rapid Dissolution of $BaSO_4$ by Macropa, an 18-Membered Macrocycle with High Affinity for Ba^{2+}

Nikki A. Thiele, Samantha N. MacMillan, and Justin J. Wilson*

Department of Chemistry and Chemical Biology, Baker Laboratory, Cornell University, Ithaca, New York 14853, United States

Supporting Information

ABSTRACT: Insoluble $BaSO_4$ scale is a costly and time-consuming problem in the petroleum industry. Clearance of $BaSO_4$-impeded pipelines requires chelating agents that can efficiently bind Ba^{2+}, the largest nonradioactive +2 metal ion. Due to the poor affinity of currently available chelating agents for Ba^{2+}, however, the dissolution of $BaSO_4$ remains inefficient, requiring very basic solutions of ligands. In this study, we investigated three diaza-18-crown-6 macrocycles bearing different pendent arms for the chelation of Ba^{2+} and assessed their potential for dissolving $BaSO_4$ scale. Remarkably, the bis-picolinate ligand macropa exhibits the highest affinity reported to date for Ba^{2+} at pH 7.4 (log K' = 10.74), forming a complex of significant kinetic stability with this large metal ion. Furthermore, the $BaSO_4$ dissolution properties of macropa dramatically surpass those of the state-of-the-art ligands DTPA and DOTA. Using macropa, complete dissolution of a molar equivalent of $BaSO_4$ is reached within 30 min at room temperature in pH 8 buffer, conditions under which DTPA and DOTA only achieve 40% dissolution of $BaSO_4$. When further applied for the dissolution of natural barite, macropa also outperforms DTPA, showing that this ligand is potentially valuable for industrial processes. Collectively, this work demonstrates that macropa is a highly effective chelator for Ba^{2+} that can be applied for the remediation of $BaSO_4$ scale.

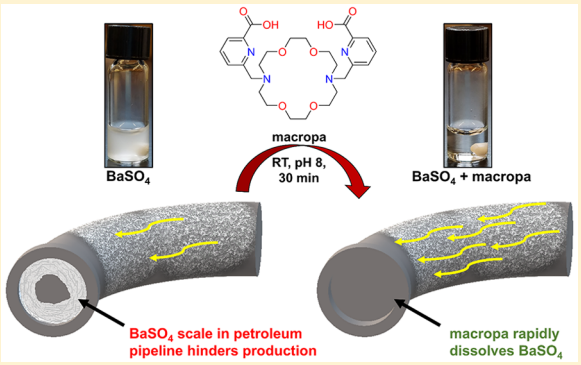

INTRODUCTION

Barium, the 14th most abundant element in the earth's crust, is the heaviest and largest nonradioactive alkaline earth (AE) metal.[1,2] Administered as a suspension of $BaSO_4$, this element has been employed for over a century as a contrast agent for X-ray imaging of the gastrointestinal tract.[3] The insolubility of $BaSO_4$ ($K_{sp} = 1.08 \times 10^{-10}$)[4] is essential for its use in medicine because it prevents this toxic heavy metal from being absorbed into the body. This same physical property, however, presents a serious problem in the industrial sector. Precipitation of $BaSO_4$ occurs frequently in oil field and gas production operations. When Ba^{2+}-rich formation waters mix with SO_4^{2-}-rich seawater, an intractable scale of $BaSO_4$ is deposited, obstructing downhole pipes and surface equipment.[5] As such, $BaSO_4$ scale is a major economic burden to the petroleum industry that slows or halts production and requires costly scale removal efforts.[6,7] In addition, the scale poses a significant health hazard to petroleum workers. Naturally occurring radioactive material (NORM), particularly long-lived bone-seeking Ra^{2+} ions, is readily incorporated into $BaSO_4$ and is mobilized during scale remediation, exposing humans to toxic levels of radioactivity.[8,9] Hence, the efficient and safe removal of $BaSO_4$ scale is of global significance.

The elimination of $BaSO_4$ scale is achieved by solubilization using chelating agents.[10−14] One of the most commonly used chelators is the acyclic ligand DTPA (Chart 1).[12] The thermodynamic stabilities of DTPA complexes of the AEs, however, decrease with increasing ionic radius of the metal ion, rendering DTPA a relatively low-affinity ligand for Ba^{2+} (log K_{BaL} = 8.78).[15] Extreme conditions of high pH (pH > 11) and heat are required to efficiently remove scale using DTPA,[16−18] reflecting the fact that this ligand is not optimal for the chelation of Ba^{2+}. The tetraaza macrocycle DOTA (Chart 1) has also been investigated for the dissolution of $BaSO_4$.[12] Despite having the highest reported thermodynamic affinity for Ba^{2+} in aqueous solution (log K_{BaL} = 11.75),[19−21] DOTA dissolves $BaSO_4$ less efficiently than DTPA,[22] reflecting the slow metal-binding kinetics of this macrocycle. Collectively, these limitations underscore the necessity to develop new ligands for Ba^{2+}.

Despite the need for new, more effective Ba^{2+} chelators for the removal of $BaSO_4$ scale, few efforts to date have been directed toward this objective.[23−25] The development of improved chelators for Ba^{2+} has further been hindered by the lack of fundamental coordination chemistry studies of this ion.[26] A key challenge for the chelation of Ba^{2+} arises from the fact that the large AEs engage primarily in ionic, rather than covalent, binding interactions with ligands. The strength of these ionic bonds is proportional to the charge-to-size ratio of the metal center, with smaller ratios giving rise to weaker electrostatic interactions. As the largest nonradioactive +2 ion

Received: August 13, 2018
Published: November 28, 2018

DOI: 10.1021/jacs.8b08704
J. Am. Chem. Soc. 2018, 140, 17071−17078

Chart 1. Structures of the Ligands Discussed in this Work

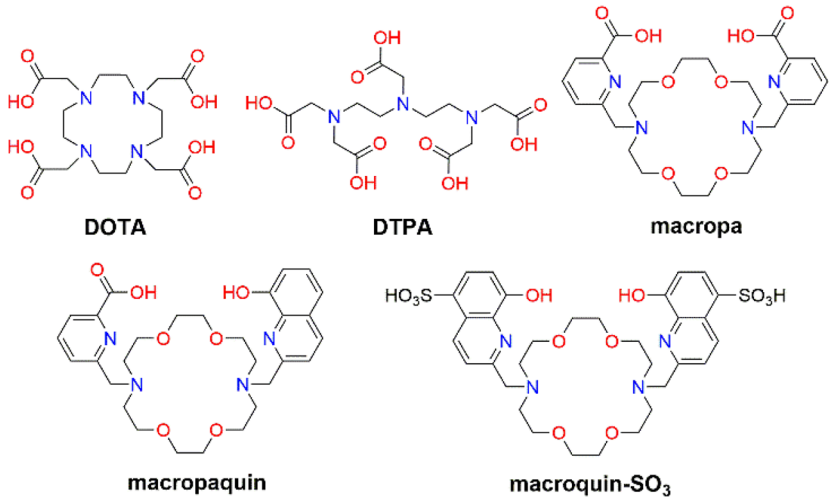

in the Periodic Table (6-coordinate ionic radius = 1.35 Å),[2] Ba^{2+} has a low charge density, resulting in coordination complexes of lower stability compared to the smaller AEs. As a result, the selective, rapid, and stable chelation of Ba^{2+} has remained elusive.

Based on our success in using the expanded 18-membered macrocycle macropa (Chart 1) for the chelation of the largest +3 ion, actinium (6-coordinate ionic radius = 1.12 Å),[27−29] we investigated the suitability of this ligand for the large Ba^{2+} ion. Additionally, two novel ligands, macropaquin and macroquin−SO_3 (Chart 1), were evaluated to systematically probe the influence of varying the metal-binding pendent arms on Ba^{2+} coordination. Our studies show that macropa has the highest affinity for Ba^{2+} at pH 7.4 reported to date, to the best of our knowledge. This ligand also possesses excellent selectivity for large over small AEs, a feature that is not observed for conventional ligands such as DTPA and DOTA. Furthermore, macropa exhibits superior $BaSO_4$ dissolution properties relative to DTPA and DOTA, rapidly solubilizing $BaSO_4$ under mild conditions. These results reveal macropa to be an exceptional chelator for the large Ba^{2+} ion and establish proof-of-concept for its industrial application as a scale dissolver, demonstrating that fundamental coordination chemistry principles can be applied to satisfy unmet societal needs.

RESULTS AND DISCUSSION

Previous studies have shown that macropa selectively binds large over small metal ions;[27,30,31] notably, the affinity of macropa for Sr^{2+} (log K_{SrL} = 9.57) is 4 orders of magnitude higher than for the smaller Ca^{2+} ion (log K_{CaL} = 5.25).[32] Based on these findings, we hypothesized that macropa may possess even higher affinity for Ba^{2+}. Macroquin, a ligand in which the picolinate pendent arms of macropa are replaced with 8-hydroxyquinoline groups, has also been investigated.[33] Ligands of this class are highly selective for Ba^{2+} over smaller AEs, although this selectivity has only been demonstrated in organic solvents owing to the poor aqueous solubility of these ligands.[33−35] To increase aqueous solubility, we installed sulfonate groups onto the 8-hydroxyquinoline arms of the macrocycle, generating macroquin−SO_3. Finally, to investigate potential metal-binding synergy between the two types of pendent arms, the mixed variant, macropaquin, was synthesized by the stepwise installation of one picolinate group and one 8-hydroxyquinoline group onto the diaza-18-crown-6 backbone. Details of the synthesis and characterization of the ligands are provided in the Supporting Information, (Figures S1−S4, S9−S12).

To probe the fundamental coordination chemistry of these ligands with Ba^{2+}, their complexes with this ion were prepared (Figures S5−S8, S13, S14) and analyzed by X-ray crystallography to elucidate their solid-state structures (Figure 1, Tables S1−S4). In each complex, the Ba^{2+} ion is situated slightly above the diaza-18-crown-6 ring, and the two pendent arms are oriented on the same side of the macrocycle. The coordination sphere of the Ba^{2+} ion comprises all 10 donor atoms of each ligand (N_4O_6), together with an oxygen atom from a coordinated solvent molecule that penetrates each macrocycle from the opposite face. Similar 11-coordinate arrangements were observed for the Ba^{2+} complexes of BHEE-18-aneN_2O_4, a diaza-18-crown-6 macrocycle bearing two pendent $-CH_2CH_2OCH_2CH_2OH$ arms,[36,37] and macroquin−Cl, in which the sulfonate groups of macroquin−SO_3 are replaced by chlorine atoms.[34]

The ligand conformation, which can be denoted with Δ or Λ to indicate the pendent arm helical twist and δ or λ to indicate the tilt of each five-membered chelate ring,[38] is identical for the three complexes. Each ligand attains the $\Delta(\delta\lambda\delta)(\delta\lambda\delta)$ conformation, present in equal amounts with its enantiomer. For complexes of macropa with other large metal ions, this conformation is also the most stable.[30,32] Protonation of one picolinate arm of macropa and the 8-hydroxyquinoline arm of macropaquin gives rise to complexes of the cationic formulas $[Ba(Hmacropa)(DMF)]^+$ and $[Ba(Hmacropaquin)(DMF)]^+$, respectively. By contrast, macroquin−SO_3 forms a neutral complex with Ba^{2+}, $[Ba(H_2macroquin{-}SO_3)(H_2O)]$. In this case, both phenolates are protonated to form neutral donors, but the sulfonic acid groups exist in the deprotonated anionic form. As reflected by the similar distances between Ba^{2+} and the two nitrogen atoms of each macrocycle, the Ba^{2+} ion is situated symmetrically within the macrocycle of each complex. Collectively, the structural features of these complexes suggest that macropa, macropaquin, and macroquin−SO_3 can optimally accommodate the large Ba^{2+} ion.

To further evaluate the coordination properties of the ligands with the AEs, their protonation constants and the stability constants of their Ca^{2+}, Sr^{2+}, and Ba^{2+} complexes were

DOI: 10.1021/jacs.8b08704
J. Am. Chem. Soc. 2018, 140, 17071−17078

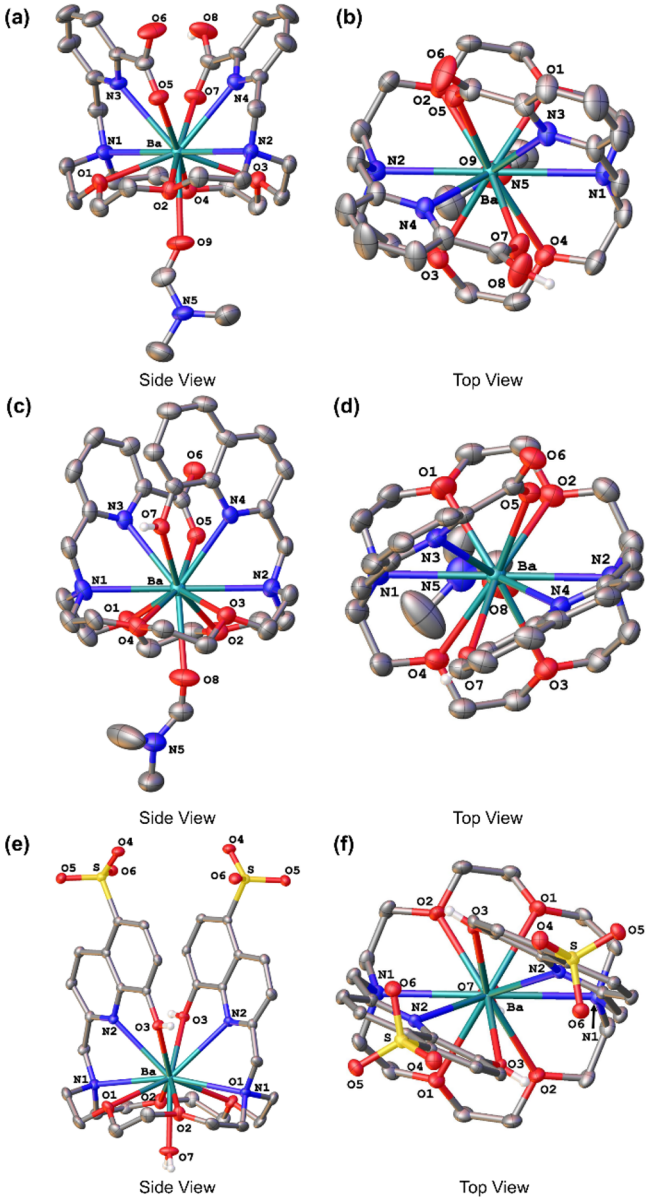

Figure 1. X-ray crystal structures of $[Ba(Hmacropa)(DMF)]ClO_4 \cdot Et_2O$ (a,b), $[Ba(Hmacropaquin)(DMF)]ClO_4 \cdot DMF$ (c,d), and $[Ba(H_2macroquin{-}SO_3)(H_2O)] \cdot 4H_2O$ (e,f). Ellipsoids are drawn at the 50% probability level. Counteranions, nonacidic hydrogen atoms, and outer-sphere solvent molecules are omitted for clarity.

measured by potentiometric titration in 0.1 M KCl (Table 1, Figures S15–S17). For comparison, corresponding values for DTPA and DOTA, the current state of the art for Ba^{2+} chelation, are also provided. The protonation constants of the ligands are defined in eq 1. The stability constants and protonation constants of the metal complexes are expressed in eqs 2 and 3, respectively.

$$K_{ai} = \frac{[H_iL]}{[H_{i-1}L][H^+]} \quad (1)$$

$$K_{ML} = \frac{[ML]}{[M][L]} \quad (2)$$

$$K_{MH_iL} = \frac{[MH_iL]}{[MH_{i-1}L][H^+]} \quad (3)$$

A comparison of the ligand protonation constants reveals that sequential replacement of each picolinate arm of macropa by 8-hydroxyquinoline-based binding groups significantly decreases the basicity of the nitrogen atoms of the macrocyclic core to which they are attached. This trend is evidenced by the lower amine protonation constants of 7.15 (log K_{a2}) and 6.97 (log K_{a3}) for macropaquin and 6.75 (log K_{a3}) and 6.62 (log K_{a4}) for macroquin–SO_3 versus 7.41 (log K_{a1}) and 6.899 (log K_{a2}) for macropa. A comparison between related ethylenediamine-derived ligands bearing either picolinate or 8-hydroxyquinoline groups also shows that the basicity of the secondary amines is lower when attached to the latter.[39,40] The electron-withdrawing sulfonate groups on macroquin–SO_3 give rise to more acidic phenols (log K_{a1} = 9.34, log K_{a2} = 9.43) compared to macropaquin (log K_{a1} = 10.33). Notably, the second protonation constant of macroquin–SO_3 is slightly larger than the first protonation constant. This apparent reversal in expected values may be attributed to intramolecular hydrogen bonding that stabilizes the second proton; upon its removal, the hydrogen-bond network is broken, and the final remaining proton becomes more acidic. This phenomenon has been previously reported for other macrocyclic ligands.[41,42]

Because protons compete with metal ions for binding sites on ligands, ligand basicity is an important factor that contributes to the affinity of a ligand for a metal ion at a specific pH.[43,44] The overall basicity of the ligands, taken as the sum of their log K_a values, follows the order macropa (19.99) < macropaquin (27.69) < macroquin–SO_3 (32.14). The speciation of the ligands reflects these overall basicity values. At pH 7.4, 43% of macropa is fully deprotonated (L^{2-}), consistent with the lower overall basicity of this ligand (Figure S18). By contrast, fully deprotonated macropaquin^{2-} and macroquin–SO_3^{4-} do not exist in solution below pH 8 (Figures S19 and S20). At pH 7.4, the monoprotonated species of macropaquin, HL^-, predominates (56%), whereas macroquin–SO_3 is mostly present as H_2L^{2-} (78%). On the basis of these results, macropaquin and macroquin–SO_3 may chelate metal ions less effectively than macropa near neutral pH due to greater competition with protons for binding sites on these ligands.

With the protonation constants in hand, the stability constants of these ligands with Ca^{2+}, Sr^{2+}, and Ba^{2+} were determined. Remarkably, macropa, macropaquin, and macroquin–SO_3 all exhibit significant thermodynamic preferences for large over small AEs; the measured log K_{ML} values are highest for complexes of Ba^{2+} and lowest for complexes of Ca^{2+}. However, the affinities of the ligands for Ba^{2+} and Sr^{2+} decrease as the picolinate arms on the macrocyclic scaffold are replaced with 8-hydroxyquinoline or 8-hydroxyquinoline-5-sulfonic acid arms. For example, log K_{BaL} values of 11.11, 10.87, and 10.44 were measured for complexes of macropa, macropaquin, and macroquin–SO_3, respectively, containing zero, one, and two 8-hydroxyquinoline-based pendent arms. This trend signifies that 8-hydroxyquinoline-based pendent arms may not be suitable metal-binding groups for the chelation of large metal ions such as Ba^{2+}.

Refinement of our potentiometric titration data also revealed the presence of protonated metal complexes, or MHL and MH_2L species, for all three ligands bound to Ca^{2+}, Sr^{2+}, and Ba^{2+} (Table 1 and Figures S21–S26). The inclusion of these species within our solution phase model is consistent with the results from X-ray crystallography, which also identified them in the solid state (Figure 1). The speciation diagrams for

DOI: 10.1021/jacs.8b08704
J. Am. Chem. Soc. 2018, 140, 17071–17078

Table 1. Protonation Constants of Macropa^{2-}, Macropaquin^{2-}, and Macroquin−SO_3^{4-} and Thermodynamic Stability Constants of Their Alkaline Earth Complexes Determined by pH Potentiometry (25 °C and I = 0.1 M KCl)[a]

	macropa^{2-}	macropaquin^{2-}	macroquin−SO_3^{4-}	DOTA^{4-}[b]	DTPA^{5-}[c]
log K_{a1}	7.41(1), [7.41][d]	10.33(4)	9.34(4)	11.14	10.34
log K_{a2}	6.899(3), [6.85][d]	7.15(3)	9.43(1)	9.69	8.59
log K_{a3}	3.23(1), [3.32][d]	6.97(2)	6.75(4)	4.85	4.25
log K_{a4}	2.45(5), [2.36][d]	3.24(4)	6.62(4)	3.95	2.71
log K_{a5}	[1.69][d]				2.18
log K_{CaL}	5.79(1), [5.25][e]	5.90(4)	6.04(8)	16.37	11.77
log K_{CaHL}		8.59(2)	8.60(4)	3.60	6.10
log K_{SrL}	9.442(4), [9.57][e]	9.19(5)	8.62(2)	14.38	9.68
log K_{SrHL}	3.35(8), [4.16][e]	8.92(2)	8.34(4)	4.52	5.4
log K_{SrH_2L}			6.920(3)		
log K_{BaL}	11.11(4)	10.87(2)	10.44(6)	11.75	8.78
log K_{BaHL}	3.76(2)	9.76(2)	9.24(7)		5.34
log K_{BaH_2L}	2.49(7)	3.28(2)	7.80(2)		

[a]Data reported previously for DOTA^{4-} and DTPA^{5-} are provided for comparison. [b]Ref 21, I = 0.1 M KCl. [c]Protonation constants and Ca^{2+} stability constants from ref 45, I = 0.1 M KCl. Other values from ref 15. [d]Ref 30, I = 0.1 M KCl. [e]Ref 32, I = 0.1 M KNO_3.

solutions of Ba^{2+} and the three ligands, based on the thermodynamic constants in Table 1, are shown in Figure 2. The major species present at pH 7.4 is the ML species for macropa, the MHL species for macropaquin, and the MH_2L species for macroquin−SO_3. These data indicate that the 8-hydroxyquinoline donors retain their basicity when bound to the Ba^{2+} ion. The presence of two such donors in macroquin−SO_3 gives rise to the large prevalence of the protonated complex MH_2L near neutral pH.

In comparing the thermodynamic properties of these ligands to the commonly employed ligands DOTA and DTPA, it is noteworthy that the log K_{BaL} value of 11.11 for macropa is substantially larger than that for DTPA (log K_{BaL} = 8.78) and only 0.64 log units lower than that for DOTA (log K_{BaL} = 11.75), indicating that macropa is a high-affinity ligand for Ba^{2+}. A more accurate reflection of thermodynamic affinity in aqueous solution, however, can be expressed using conditional stability constants, which account for the effect of protonation equilibria of the ligands on complex stability.[46,47] The conditional stability constants (log K') of the AE complexes at pH 7.4 are given in Table 2. The log K'_{Ba} value of 10.74 for macropa is 5−6 orders of magnitude greater than those for DOTA (log K'_{Ba} = 5.72) and DTPA (log K'_{Ba} = 4.63). Macropa also exhibits higher affinity for Ba^{2+} at pH 7.4 than macropaquin (log K'_{Ba} = 10.05) and macroquin−SO_3 (log K'_{Ba} = 8.76). From these values, macropa emerges as remarkably superior to all other ligands for the chelation of Ba^{2+} at near-neutral pH.

Another measure of conditional thermodynamic affinity of a ligand for a metal ion is provided by pM values (Table 2), which are defined as the negative log of the free metal concentration in a pH 7.4 solution containing 10^{-6} M metal ion and 10^{-5} M ligand.[48] Larger pM values correspond to higher affinity chelators because they indicate that there is a smaller concentration of free metal ion under these conditions at equilibrium. The pBa values of DOTA and DTPA are only 6.76 and 6.15, respectively, reflecting the presence of a significant amount of free Ba^{2+} at pH 7.4 (Figure 2). By contrast, 90% of Ba^{2+} is already bound by macropa at pH 4.0 and 99% is complexed at pH 5.1, consistent with the high pBa value of 11.69 for this ligand. Furthermore, macropa is 1.17-fold and 1.79-fold more selective for Ba^{2+} over Sr^{2+} and Ca^{2+}, respectively, as determined by the ratio of the corresponding pM values. By contrast, these selectivity values are <1 for DOTA and DTPA, emphasizing their poor affinities for the large Ba^{2+} ion at pH 7.4.

Having demonstrated that macropa chelates Ba^{2+} with high thermodynamic stability and selectivity, the kinetic inertness of this complex was examined in comparison to that of macropaquin and macroquin−SO_3. We first challenged the Ba−L complexes with 1000 equiv of La^{3+}, a metal that forms a complex of high thermodynamic stability with macropa (log K_{LaL} = 14.99).[30] The substitution of Ba^{2+} with La^{3+} was monitored at room temperature (RT) and pH 7.3 by UV−vis spectrophotometry (Figures S27−S29). Ba−macropa and Ba−macropaquin exhibited moderate stability, giving rise to similar half-lives of 5.45 ± 0.20 min and 6.07 ± 0.13 min, respectively. By contrast, Ba−macroquin−SO_3 underwent transmetalation with La^{3+} much more rapidly ($t_{1/2}$ = 0.65 ± 0.05 min), indicating that macroquin−SO_3 cannot adequately retain Ba^{2+} under these conditions.

Because Ba^{2+} possesses bone-seeking properties, the stability of the Ba^{2+} complexes in the presence of hydroxyapatite ($Ca_5(PO_4)_3(OH)$, HAP), the predominant mineral that comprises bone, was also evaluated.[49,50] HAP was suspended in solutions containing the complexes formed in situ (1.1 equiv L, 1.0 equiv Ba^{2+}) in pH 7.6 buffer, and the amount of Ba^{2+} remaining in the liquid phase, reflecting intact Ba−L complex, was determined by graphite furnace atomic absorption spectroscopy (GFAAS) (Figure S30). Whereas free Ba^{2+} is adsorbed by HAP in <10 min, Ba−macropa and Ba−macropaquin, respectively, retained 82% and 68% of this ion after 20 h. Ba−macroquin−SO_3 displayed the least stability in the presence of HAP, with only 17% of the complex remaining intact after 20 h. Taken together, the results of these challenges demonstrate that Ba−macropa and Ba−macropaquin are considerably more stable than Ba−macroquin−SO_3 under extreme conditions of large excesses of competing metal ions. This feature may be important for Ba^{2+} chelation in industrial applications, such as scale dissolution, because numerous other metal ions are present during these processes. The inferior kinetic stability of Ba−macroquin−SO_3 relative to the other two complexes correlates with the lower thermodynamic affinity of this ligand for Ba^{2+} and is most likely a consequence of the fact that the diprotonated Ba^{2+} complex of macroquin−SO_3, MH_2L, is the major species at pH 7.4 (Figure 2). This

DOI: 10.1021/jacs.8b08704
J. Am. Chem. Soc. 2018, 140, 17071−17078

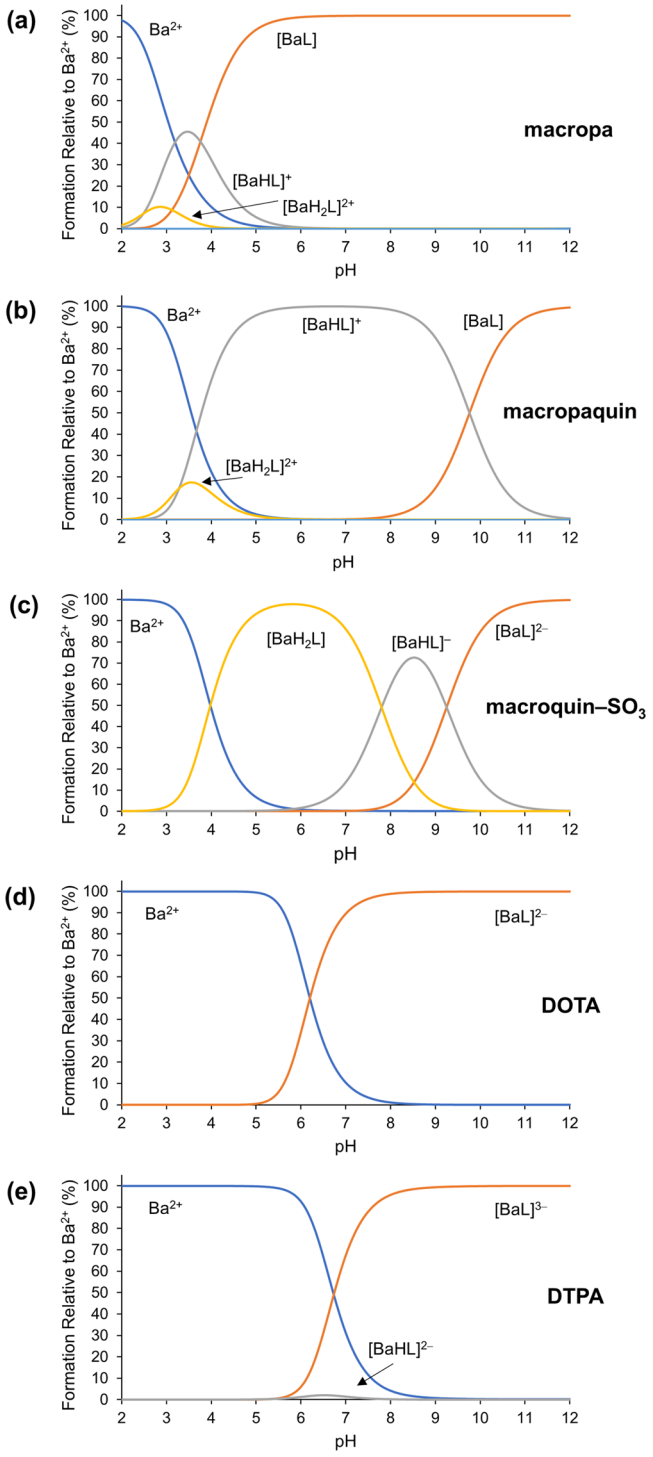

Figure 2. Species distribution diagrams of (a) macropa, (b) macropaquin, (c) macroquin–SO_3, (d) DOTA, and (e) DTPA in the presence of Ba^{2+} at $[Ba^{2+}]_{tot} = [L]_{tot} = 1.0$ mM, $I = 0.1$ M KCl, and 25 °C.

complex is expected to be substantially more labile than the ML species due to decreased electrostatic interactions between the ion and ligand.

The encouraging results of the thermodynamic and kinetic stability studies prompted us to evaluate the feasibility of employing macropa and macropaquin as $BaSO_4$ scale dissolvers. First, a suspension of $BaSO_4$ in pH 8 $NaHCO_3$ was formed by combining $Ba(NO_3)_2$ (4.53 mM) with excess

Table 2. Conditional Stability Constants (log K')[a] and pM Values[b] at pH 7.4 for the Alkaline Earth Complexes of the Ligands Discussed

	macropa	macropaquin	macroquin–SO_3	DOTA	DTPA
log K'_{Ca}	5.42	3.94	3.19	10.34	7.63
log K'_{Sr}	9.07	7.54	5.64	8.35	5.53
log K'_{Ba}	10.74	10.05	8.76	5.72	4.63
pCa	6.54	6.04	6.01	11.29	8.59
pSr	10.02	8.50	6.70	9.30	6.61
pBa	11.69	11.01	9.72	6.76	6.15

[a]Conditional stability constants at pH 7.4, 25 °C, and $I = 0.1$ M KCl. [b]Calculated from $-\log [M^{2+}]_{free}$ ($[M^{2+}]_{tot} = 10^{-6}$ M; $[L]_{tot} = 10^{-5}$ M; pH 7.4; 25 °C; $I = 0.1$ M KCl).

Na_2SO_4 (13.48 mM), simulating the mixing of incompatible waters that produces $BaSO_4$ scale in petroleum operations. The resulting $BaSO_4$ suspension was treated with ligand (5 mM), and the amount of dissolved Ba^{2+} was measured by GFAAS (Figure 3). Macropa rapidly solubilized 78% of $BaSO_4$ in just

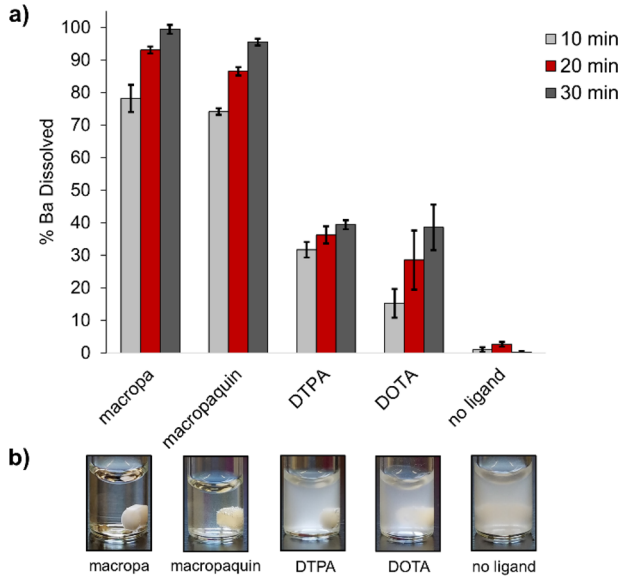

Figure 3. Dissolution of $BaSO_4$ by macropa, macropaquin, DTPA, and DOTA. (a) Dissolution at RT and pH 8 was initiated by the addition of chelator (5 mM) to a suspension of $BaSO_4$ (4.53 mM $Ba(NO_3)_2$ and 13.48 mM Na_2SO_4). Barium content in solution was measured by GFAAS after 10, 20, and 30 min. (b) Samples from dissolution experiments after 30 min.

10 min and afforded complete dissolution after 30 min. Likewise, macropaquin dissolved 95% of $BaSO_4$ in 30 min. By contrast, the conventional ligands DOTA and DTPA dissolved only 40% of $BaSO_4$ within this same time, underscoring the inferior solubilizing properties of these ligands at pH 8.

The dissolution of $BaSO_4$ by macropa, DTPA, and DOTA was further evaluated in pH 11 Na_2CO_3 buffer (Figure S31) to match the caustic conditions that are applied in the industrial setting. Impressively, macropa solubilized >95% of the $BaSO_4$ in just 5 min. DTPA also dissolved nearly all the $BaSO_4$ in this same time. The improved dissolution ability of DTPA at pH 11 versus pH 8 reflects the greater proportion of the fully deprotonated ligand ($DTPA^{5-}$) present at pH 11, which favors Ba–DTPA complex formation. These results are consistent with the fact that the petroleum industry only uses this ligand

DOI: 10.1021/jacs.8b08704
J. Am. Chem. Soc. 2018, 140, 17071−17078

under conditions of high pH.[16−18] The similar rates at which macropa and DTPA solubilize $BaSO_4$ at pH 11 suggest that macropa possesses remarkably fast Ba^{2+}-binding kinetics. The macrocycle DOTA, by contrast, was unable to completely dissolve all the $BaSO_4$. After 30 min, only 75% dissolution was reached, signifying that the kinetics of metal incorporation for DOTA remain slow even at high pH.

We next investigated the ligand-promoted dissolution of crude barite ore, which is composed predominately of $BaSO_4$, as a model for the solid deposits of natural scale that plague the petroleum industry. Barite rocks (Figure 4a) obtained from Excalibar Minerals (Katy, TX) were milled and sieved to isolate particles between 0.5 and 2 mm (Figure 4b). To simulate production tubing clogged with $BaSO_4$ scale, polypropylene columns were filled with barite (3 g), to which solutions of macropa or DTPA at pH 8 or 11 were added (Figure 4c). The concentration of each ligand solution was approximately 48 mM, consistent with the dilute compositions of scale dissolvers used industrially.[11,13,16,18,51] After a soak time of 1 h, the ligand solution was eluted from the column, and the concentration of dissolved barium was measured by GFAAS and converted to ligand efficiency (eq 4).

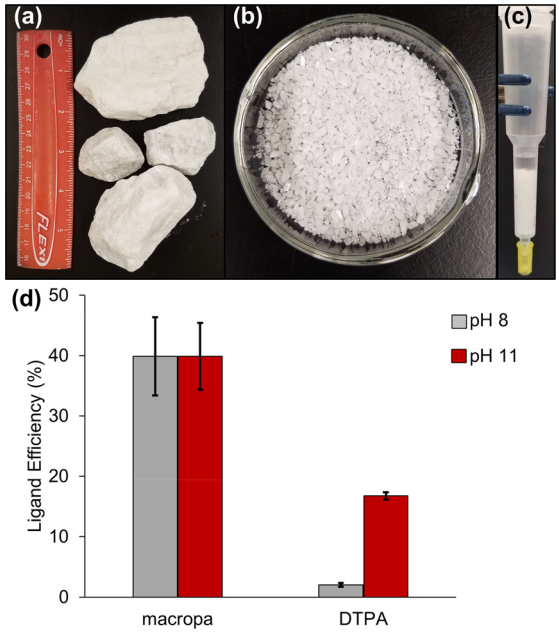

Figure 4. Barite dissolution efficiency of macropa and DTPA. (a) Large rocks of crude barite ore were crushed with a hammer. (b) The barite was sieved to isolate particles between 0.5 and 2 mm. (c) To simulate petroleum pipes clogged with $BaSO_4$ scale, columns were filled with barite (3 g), and then solutions of macropa or DTPA (~48 mM) at pH 8 and pH 11 were added. (d) After a soak period of 1 h, ligand efficiency, or the percent of ligand saturated with Ba^{2+}, was determined by measuring the concentration of barium in the eluate by GFAAS.

$$\text{ligand efficiency} = \frac{Ba_{exp}}{Ba_{max}} \times 100 \quad (4)$$

In eq 4, Ba_{exp} is the concentration of barium measured in the eluate, and Ba_{max} is the maximum concentration of barium that can be chelated by each ligand, calculated from the concentration of each ligand applied to the column and assuming a 1:1 M:L binding model. As shown in Figure 4d, the ligand efficiency of macropa at pH 8 is 40%, indicating that nearly half of the ligand solution was saturated with Ba^{2+} following exposure to barite for 1 h. DTPA, by contrast, was practically incapable of dissolving barite at this pH, giving rise to a ligand efficiency of only 2%. Macropa remained equally as effective at pH 11, again displaying a ligand efficiency of 40%. By contrast, even at pH 11, the dissolution efficiency of DTPA was only 17%, less than half that observed for macropa. Collectively, these results indicate that macropa maximally dissolves barite at or below pH 8, underscoring its superior affinity for Ba^{2+} near neutral pH.

Lastly, the capacity for recovery and reuse of macropa post-$BaSO_4$ dissolution was assessed qualitatively (Figure 5). A sample of macropa-dissolved $BaSO_4$ (9.66 mM macropa, 8.74 mM $Ba(NO_3)_2$, 26.04 mM Na_2SO_4) was acidified to pH 1 with concentrated HCl to protonate the ligand, inducing Ba^{2+} decomplexation and precipitation as $BaSO_4$. The macropa solution was isolated by filtration, basified to pH 8 with 2 M NaOH, and combined with another portion of $BaSO_4$. Within 40 min, no visible precipitate remained in the vial, signaling that the recycled macropa dissolved all the $BaSO_4$. Subsequently, the ligand was recovered and reused for $BaSO_4$ dissolution four more times with negligible losses in efficacy or speed of dissolution (Figure S32). These results demonstrate the facile and economic reuse of macropa, an attractive feature that will facilitate its implementation in industry.[52]

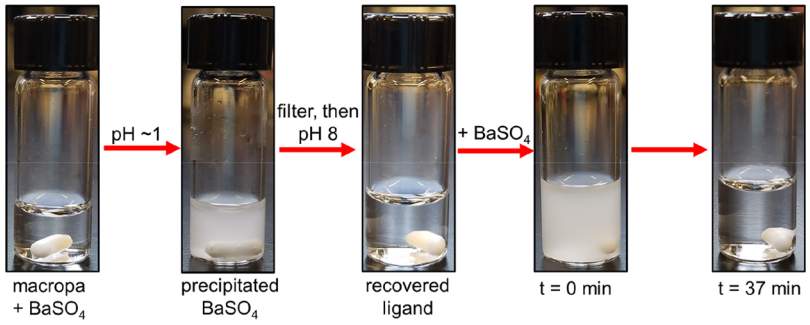

Figure 5. Ligand recovery and reuse. A solution of macropa-dissolved $BaSO_4$ was acidified to release the Ba^{2+} from the ligand as $BaSO_4$. After filtration of the precipitated $BaSO_4$ and basification of the solution, the recovered ligand was successfully reused for another cycle of $BaSO_4$ dissolution.

DOI: 10.1021/jacs.8b08704
J. Am. Chem. Soc. 2018, 140, 17071−17078

CONCLUSION

In summary, three ligands based on the expanded diaza-18-crown-6 macrocycle were evaluated for their abilities to chelate the large Ba^{2+} ion. Macropa exhibits unprecedented affinity for Ba^{2+} at pH 7.4, possessing a log K' value of 10.74. The Ba^{2+} complexes of both macropa and macropaquin display substantial kinetic stability when challenged with La^{3+} or HAP, whereas macroquin−SO_3 rapidly releases Ba^{2+} under these conditions. Additionally, macropa and macropaquin can efficiently dissolve $BaSO_4$ under RT and near-neutral pH conditions. This feature was further reflected in dissolution studies involving authentic barite ore samples, which showed macropa to be superior to the state-of-the-art chelator DTPA. The promising Ba^{2+}-chelation properties of this ligand will render it useful for the dissolution of $BaSO_4$ scale deposits, fulfilling an important unmet need in the petroleum industry.

More broadly, these results reveal key features that are required for stable coordination of the heavy AE ions. Namely, the observation that picolinate donors provide superior coordination properties for Ba^{2+} in comparison to 8-hydroxyquinoline donors will guide future ligand design efforts for this underexplored metal ion. These results have further implications in the realm of radiochemistry, where these ligands may be applied for the chelation of Ra^{2+}. Due to both concerns about radiological contamination of ^{226}Ra in NORM and the great therapeutic potential of ^{223}Ra for the treatment of cancer, a better understanding of AE chemistry will advance efforts to chelate Ra^{2+} for these important applications.

ASSOCIATED CONTENT

Supporting Information

The Supporting Information is available free of charge on the ACS Publications website at DOI: 10.1021/jacs.8b08704.

Experimental details, compound characterization, and supporting figures and tables (PDF)

Crystallographic information (CIF)

AUTHOR INFORMATION

Corresponding Author

*jjw275@cornell.edu

ORCID

Justin J. Wilson: 0000-0002-4086-7982

Funding

This work was supported by Cornell University and by a Pilot Award from the Weill Cornell Medical College Clinical and Translational Science Center, funded by NIH/NCATS UL1TR00457. This research made use of the NMR Facility at Cornell University, which is supported in part by the NSF under award number CHE-1531632.

Notes

The authors declare the following competing financial interest(s): N.A.T. and J.J.W. have filed a provisional patent on the application of this class of ligands for $BaSO_4$ scale dissolution.

ACKNOWLEDGMENTS

The authors thank Dr. Vojtěch Kubíček (Charles University, Prague, The Czech Republic) for his valuable guidance with potentiometry and Excalibar Minerals (Katy, TX) for providing us with a sample of barite ore.

REFERENCES

(1) Beryllium, Magnesium, Calcium, Strontium, Barium and Radium. In *Chemistry of the Elements*, 2nd ed.; Greenwood, N., Earnshaw, A., Eds.; Butterworth-Heinemann: Oxford, 1997; pp 107−138.

(2) Shannon, R. D. *Acta Crystallogr., Sect. A: Cryst. Phys., Diffr., Theor. Gen. Crystallogr.* **1976**, *32*, 751−767.

(3) Schott, G. D. *Med. Hist.* **1974**, *18*, 9−21.

(4) *CRC Handbook of Chemstry and Physics*, 87th ed.; Lide, D. R., Ed.; CRC Press: Boca Raton, FL, 2006.

(5) Li, J.; Tang, M.; Ye, Z.; Chen, L.; Zhou, Y. *J. Dispersion Sci. Technol.* **2017**, *38*, 661−670.

(6) Clemmit, A. F.; Ballance, D. C.; Hunton, A. G. The dissolution of scales in oilfield systems, SPE14010/1. Proceedings from *Offshore Europe*, Aberdeen, UK, September 10−13, 1985; Society of Petroleum Engineers: Richardson, Texas, 1985.

(7) Crabtree, M.; Eslinger, D.; Fletcher, P.; Miller, M.; Johnson, A.; King, G. *Oilfield Rev.* **1999**, *11*, 30−45.

(8) Zielinski, R. A.; Otton, J. K. Naturally occurring radioactive materials (NORM) in produced water and oil-field equipment - An issue for the energy industry. *Fact Sheet 142-99*; U.S. Geological Survey: Reston, VA, 1999.

(9) Ghose, S.; Heaton, B. The Release of Radium from Scales Produced in the North Sea Oil Fields. In *Radioactivity in the Environment*; Simopoulos, E. S., Ed.; Elsevier: Amsterdam, The Netherlands, 2005; Vol. 7, pp 1081−1089.

(10) de Jong, F.; Reinhoudt, D. N.; Torny-Schutte, G. J.; van Zon, A. Novel macrocyclic polyethers and the use of salts thereof for dissolving barium sulfate scale. UK Patent Application GB2024822A, January 16, 1980.

(11) Lakatos, I.; Lakatos-Szabó, J.; Kosztin, B. Comparative study of different barite dissolvers: Technical and economic aspects, SPE 73719. Proceedings from the *International Symposium and Exhibition on Formation Damage Control*, Lafayette, LA, February 20−21, 2002; Society of Petroleum Engineers, Richardson, Texas, 2002.

(12) Almubarak, T.; Ng, J. H.; Nasr-El-Din, H. Oilfield scale removal by chelating agents: An aminopolycarboxylic acids review, SPE-185636-MS. Proceedings from the *SPE Western Regional Meeting*, Bakersfield, CA, April 23−27, 2017; Society of Petroleum Engineers, Richardson, Texas, 2017.

(13) Mason, D. J. Formulations and methods for mineral scale removal. U.S. Patent Appl. US20170369764A1, December 28, 2017.

(14) Mason, D. J. Composition for removing naturally occurring radioactive material (NORM) scale. U.S. Patent Appl. US20170313927A1, November 2, 2017.

(15) Martell, A. E.; Smith, R. M. *Critical Stability Constants*; Plenum Press: New York, 1974; Vol. *1*.

(16) Putnis, A.; Putnis, C. V.; Paul, J. M. The efficiency of a DTPA-based solvent in the dissolution of barium sulfate scale deposits. SPE 29094. Proceedings from the *SPE International Symposium on Oilfield Chemistry*, San Antonio, TX, February 14−17, 1995; Society of Petroleum Engineers: Richardson, Texas, 1995.

(17) Dunn, K.; Yen, T. F. *Environ. Sci. Technol.* **1999**, *33*, 2821−2824.

(18) Putnis, C. V.; Kowacz, M.; Putnis, A. *Appl. Geochem.* **2008**, *23*, 2778−2788.

(19) Stetter, H.; Frank, W.; Mertens, R. *Tetrahedron* **1981**, *37*, 767−772.

(20) Delgado, R.; Fraûsto Da Silva, J. J. R. *Talanta* **1982**, *29*, 815−822.

(21) Clarke, E. T.; Martell, A. E. *Inorg. Chim. Acta* **1991**, *190*, 27−36.

(22) Wang, K.-S.; Tang, Y.; Shuler, P. J.; Dunn, K.; Koel, B. E.; Yen, T. F. Effects of scale dissolvers on barium sulfate deposits: A macroscopic and microscopic study, Paper 02309. Proceedings from *Corrosion 2002*, Denver, CO, April 7−11, 2002; National Association of Corrosion Engineers International: Houston, TX, 2002.

(23) Boubekeur-Lecaque, L.; Souffrin, C.; Gontard, G.; Boubekeur, K.; Amatore, C. *Polyhedron* **2014**, *68*, 191−198.

(24) Steinberg, J.; Bauer, D.; Reissig, F.; Köckerling, M.; Pietzsch, H.-J.; Mamat, C. *ChemistryOpen* **2018**, *7*, 432−438.
(25) Bauer, D.; Gott, M.; Steinbach, J.; Mamat, C. *Spectrochim. Acta, Part A* **2018**, *199*, 50−56.
(26) Poonia, N. S.; Bajaj, A. V. *Chem. Rev.* **1979**, *79*, 389−445.
(27) Thiele, N. A.; Brown, V.; Kelly, J. M.; Amor-Coarasa, A.; Jermilova, U.; MacMillan, S. N.; Nikolopoulou, A.; Ponnala, S.; Ramogida, C. F.; Robertson, A. K. H.; Rodríguez-Rodríguez, C.; Schaffer, P.; Williams, C., Jr.; Babich, J. W.; Radchenko, V.; Wilson, J. J. *Angew. Chem., Int. Ed.* **2017**, *56*, 14712−14717.
(28) Thiele, N. A.; Wilson, J. J. *Cancer Biother. Radiopharm.* **2018**, *33*, 336−348.
(29) Kelly, J. M.; Amor-Coarasa, A.; Ponnala, S.; Nikolopoulou, A.; Williams, C., Jr.; Thiele, N. A.; Schlyer, D.; Wilson, J. J.; DiMagno, S. G.; Babich, J. W. *J. Nucl. Med.* **2018**, *59*, 219592.
(30) Roca-Sabio, A.; Mato-Iglesias, M.; Esteban-Gómez, D.; Tóth, É.; de Blas, A.; Platas-Iglesias, C.; Rodríguez-Blas, T. *J. Am. Chem. Soc.* **2009**, *131*, 3331−3341.
(31) Jensen, M. P.; Chiarizia, R.; Shkrob, I. A.; Ulicki, J. S.; Spindler, B. D.; Murphy, D. J.; Hossain, M.; Roca-Sabio, A.; Platas-Iglesias, C.; de Blas, A.; Rodríguez-Blas, T. *Inorg. Chem.* **2014**, *53*, 6003−6012.
(32) Ferreirós-Martínez, R.; Esteban-Gómez, D.; Tóth, É.; de Blas, A.; Platas-Iglesias, C.; Rodríguez-Blas, T. *Inorg. Chem.* **2011**, *50*, 3772−3784.
(33) Su, N.; Bradshaw, J. S.; Zhang, X. X.; Song, H.; Savage, P. B.; Xue, G.; Krakowiak, K. E.; Izatt, R. M. *J. Org. Chem.* **1999**, *64*, 8855−8861.
(34) Zhang, X. X.; Bordunov, A. V.; Bradshaw, J. S.; Dalley, N. K.; Kou, X.; Izatt, R. M. *J. Am. Chem. Soc.* **1995**, *117*, 11507−11511.
(35) Bordunov, A. V.; Bradshaw, J. S.; Zhang, X. X.; Dalley, N. K.; Kou, X.; Izatt, R. M. *Inorg. Chem.* **1996**, *35*, 7229−7240.
(36) Bhavan, R.; Hancock, R. D.; Wade, P. W.; Boeyens, J. C. A.; Dobson, S. M. *Inorg. Chim. Acta* **1990**, *171*, 235−238.
(37) Hancock, R. D.; Siddons, C. J.; Oscarson, K. A.; Reibenspies, J. M. *Inorg. Chim. Acta* **2004**, *357*, 723−727.
(38) Jensen, K. A. *Inorg. Chem.* **1970**, *9*, 1−5.
(39) Boros, E.; Ferreira, C. L.; Cawthray, J. F.; Price, E. W.; Patrick, B. O.; Wester, D. W.; Adam, M. J.; Orvig, C. *J. Am. Chem. Soc.* **2010**, *132*, 15726−15733.
(40) Wang, X.; de Guadalupe Jaraquemada-Pelaéz, M.; Cao, Y.; Pan, J.; Lin, K.-S.; Patrick, B. O.; Orvig, C. *Inorg. Chem.* **2018**, DOI: 10.1021/acs.inorgchem.8b01208.
(41) Hancock, R. D.; Motekaitis, R. J.; Mashishi, J.; Cukrowski, I.; Reibenspies, J. H.; Martell, A. E. *J. Chem. Soc., Perkin Trans. 2* **1996**, 1925−1929.
(42) Rohovec, J.; Kývala, M.; Vojtíšek, P.; Hermann, P.; Lukeš, I. *Eur. J. Inorg. Chem.* **2000**, *2000*, 195−203.
(43) Martell, A. E.; Hancock, R. D.; Motekaitis, R. J. *Coord. Chem. Rev.* **1994**, *133*, 39−65.
(44) Doble, D. M. J.; Melchior, M.; O'Sullivan, B.; Siering, C.; Xu, J.; Pierre, V. C.; Raymond, K. N. *Inorg. Chem.* **2003**, *42*, 4930−4937.
(45) Schmitt-Willich, H.; Brehm, M.; Ewers, C. L. J.; Michl, G.; Müller-Fahrnow, A.; Petrov, O.; Platzek, J.; Radüchel, B.; Sülzle, D. *Inorg. Chem.* **1999**, *38*, 1134−1144.
(46) Alberty, R. A. *Eur. J. Biochem.* **1996**, *240*, 1−14.
(47) Burgot, J.-L. Conditional Stability Constants. In *Ionic Equilibria in Analytical Chemistry*; Springer: New York, 2012; pp 485−501.
(48) Harris, W. R.; Carrano, C. J.; Raymond, K. N. *J. Am. Chem. Soc.* **1979**, *101*, 2722−2727.
(49) Li, W. P.; Ma, D. S.; Higginbotham, C.; Hoffman, T.; Ketring, A. R.; Cutler, C. S.; Jurisson, S. S. *Nucl. Med. Biol.* **2001**, *28*, 145−154.
(50) Cawthray, J. F.; Creagh, A. L.; Haynes, C. A.; Orvig, C. *Inorg. Chem.* **2015**, *54*, 1440−1445.
(51) Jordan, M. M.; Williams, H.; Linares-Samaniego, S.; Frigo, D. M. New insights on the impact of high temperature conditions (176°C) on carbonate and sulphate scale dissolver performance, SPE-169785. Proceedings from the *SPE International Oilfield Scale Conference and Exhibition*, Aberdeen, Scotland, May 14−15, 2014; Society of Petroleum Engineers: Richardson, Texas, 2014.
(52) Morris, R. L.; Paul, J. M. Method for regenerating a solvent for scale removal from aqueous systems. PCT Int. Appl. WO9206044A1, April 16, 1992.

DOI: 10.1021/jacs.8b08704
J. Am. Chem. Soc. 2018, 140, 17071−17078